iScience, Volume *25*

Supplemental information

Integrative genomic analysis reveals low T-cell infiltration as the primary feature of tobacco use in HPV-positive oropharyngeal cancer

Benjamin M. Wahle, Paul Zolkind, Ricardo J. Ramirez, Zachary L. Skidmore, Sydney R. Anderson, Angela Mazul, D. Neil Hayes, Vlad C. Sandulache, Wade L. Thorstad, Douglas Adkins, Obi L. Griffith, Malachi Griffith, and Jose P. Zevallos

Figure S1

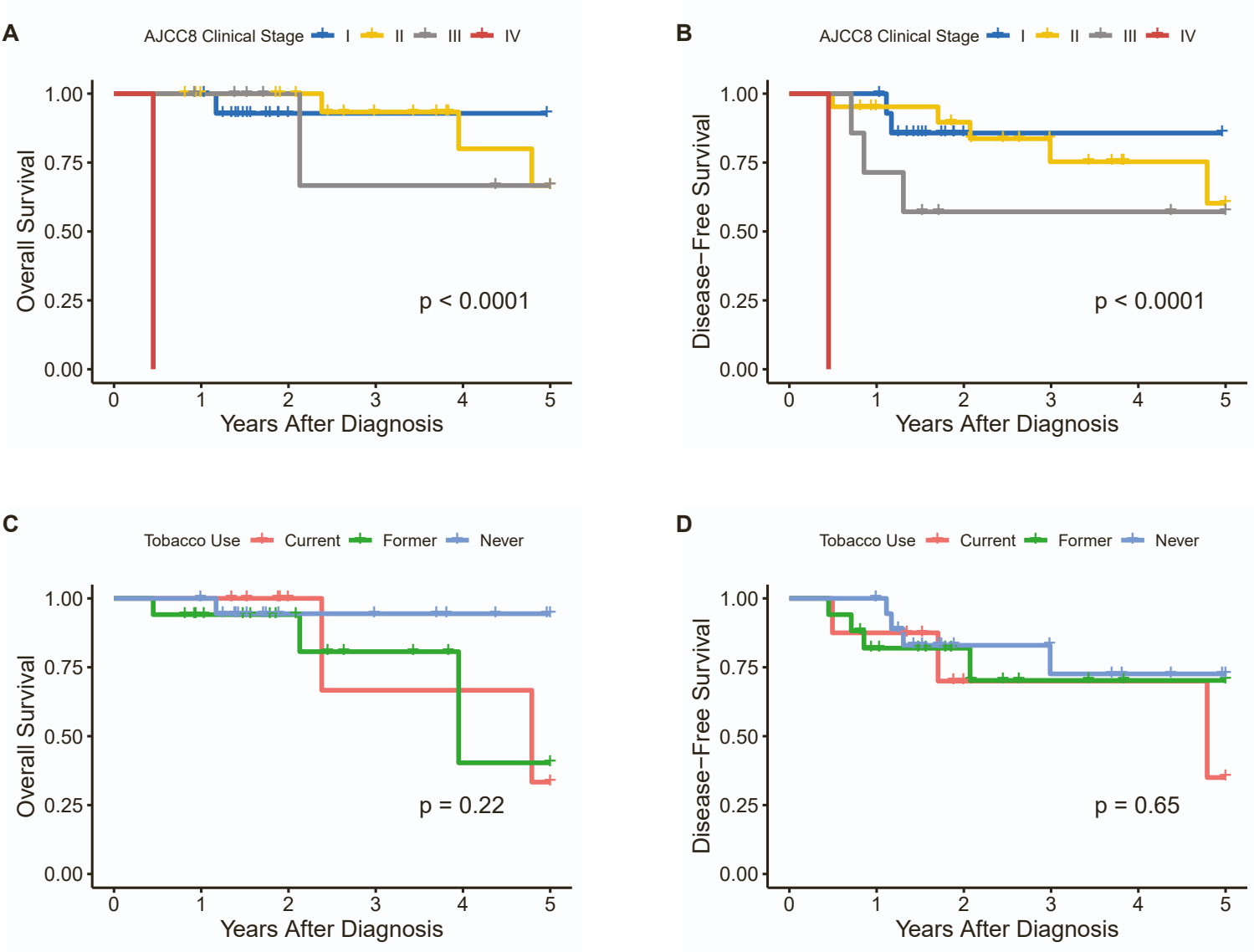
A
AJCC8 Clinical Stage I II III IV
Overall Survival
1.00
0.75
0.50
0.25
0.00
p < 0.0001
0 1 2 3 4 5
Years After Diagnosis
B
AJCC8 Clinical Stage I II III IV
Disease−Free Survival
1.00
0.75
0.50
0.25
0.00
p < 0.0001
0 1 2 3 4 5
Years After Diagnosis
C
Tobacco Use Current Former Never
Overall Survival
1.00
0.75
0.50
0.25
0.00
p = 0.22
0 1 2 3 4 5
Years After Diagnosis
D
Tobacco Use Current Former Never
Disease−Free Survival
1.00
0.75
0.50
0.25
0.00
p = 0.65
0 1 2 3 4 5
Years After Diagnosis

Figure S2

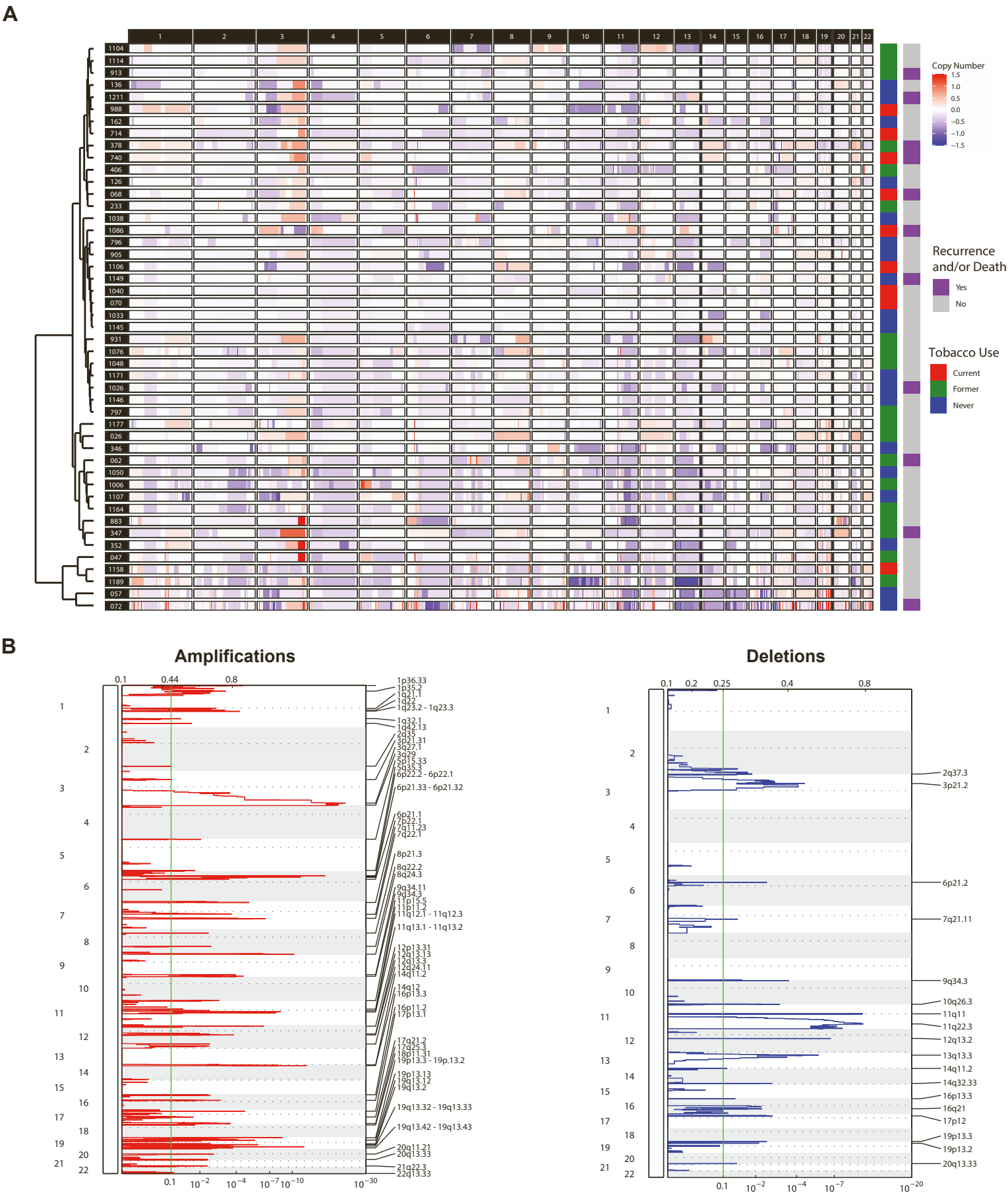
A
Copy Number
1.5
1.0
0.5
0.0
−0.5
−1.0
−1.5
Recurrence and/or Death
Yes
No
Tobacco Use
Current
Former
Never
B
Amplifications
Deletions
1p36.33
1p35.2
1q21.1
1q22
1q23.2 - 1q23.3
1q32.1
1q42.13
2q35
3p21.31
3q27.1
3q29
5p15.33
5q35.3
6p22.2 - 6p22.1
6p21.33 - 6p21.32
6p21.1
7p22.1
7q11.23
7q22.1
8p21.3
8q22.2
8q24.3
9q34.11
9q34.3
11p15.5
11p11.2
11q12.1 - 11q12.3
11q13.1 - 11q13.2
12p13.31
12q13.13
12q13.3
12q24.11
14q11.2
14q12
16p13.3
16p11.2
17p13.1
17q21.2
17q25.3
18p11.31
19p13.3 - 19p.13.2
19p13.13
19q13.12
19q13.2
19q13.32 - 19q13.33
19q13.42 - 19q13.43
20q11.21
20q13.33
21q22.3
22q13.33
2q37.3
3p21.2
6p21.2
7q21.11
9q34.3
10q26.3
11q11
11q22.3
12q13.2
13q13.3
14q11.2
14q32.33
16p13.3
16q21
17p12
19p13.3
19p13.2
20q13.33

Figure S3

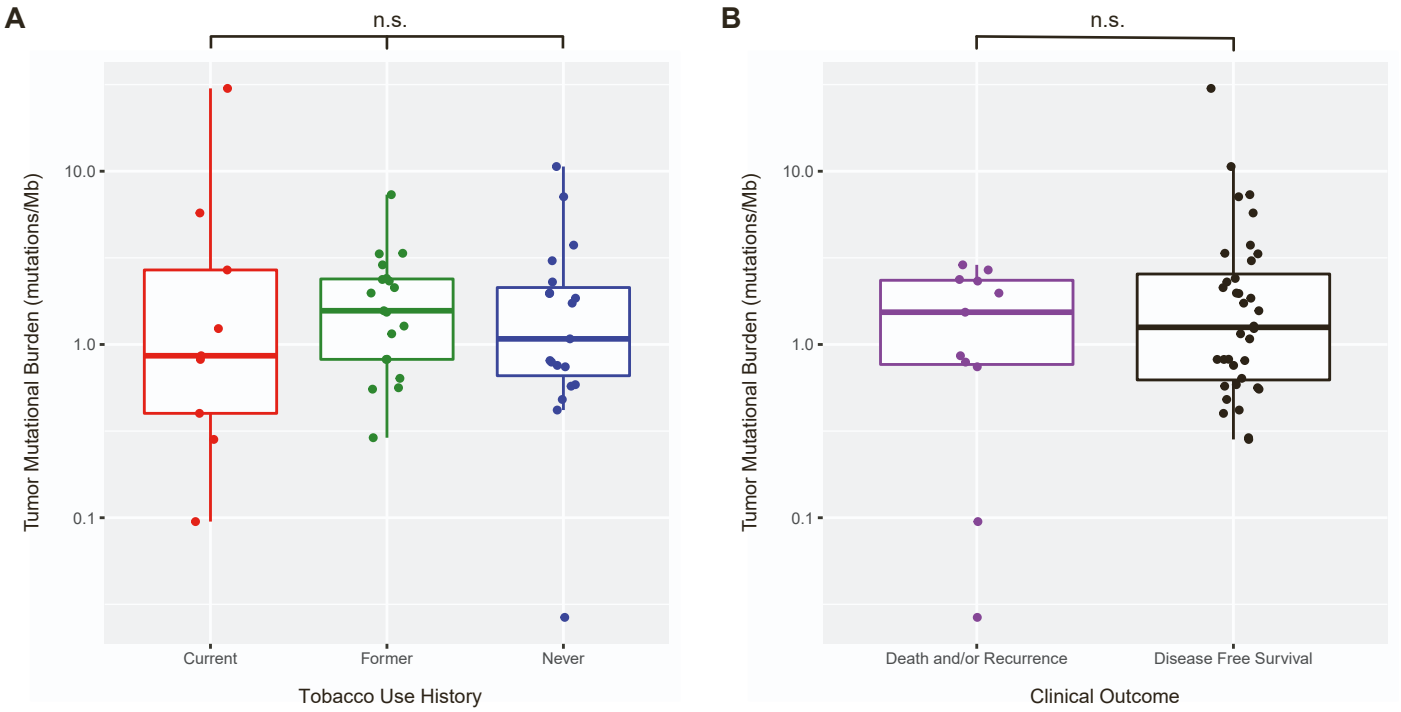
A
n.s.
10.0
1.0
0.1
Tumor Mutational Burden (mutations/Mb)
Current
Former
Never
Tobacco Use History
B
n.s.
10.0
1.0
0.1
Tumor Mutational Burden (mutations/Mb)
Death and/or Recurrence
Disease Free Survival
Clinical Outcome

Figure S4

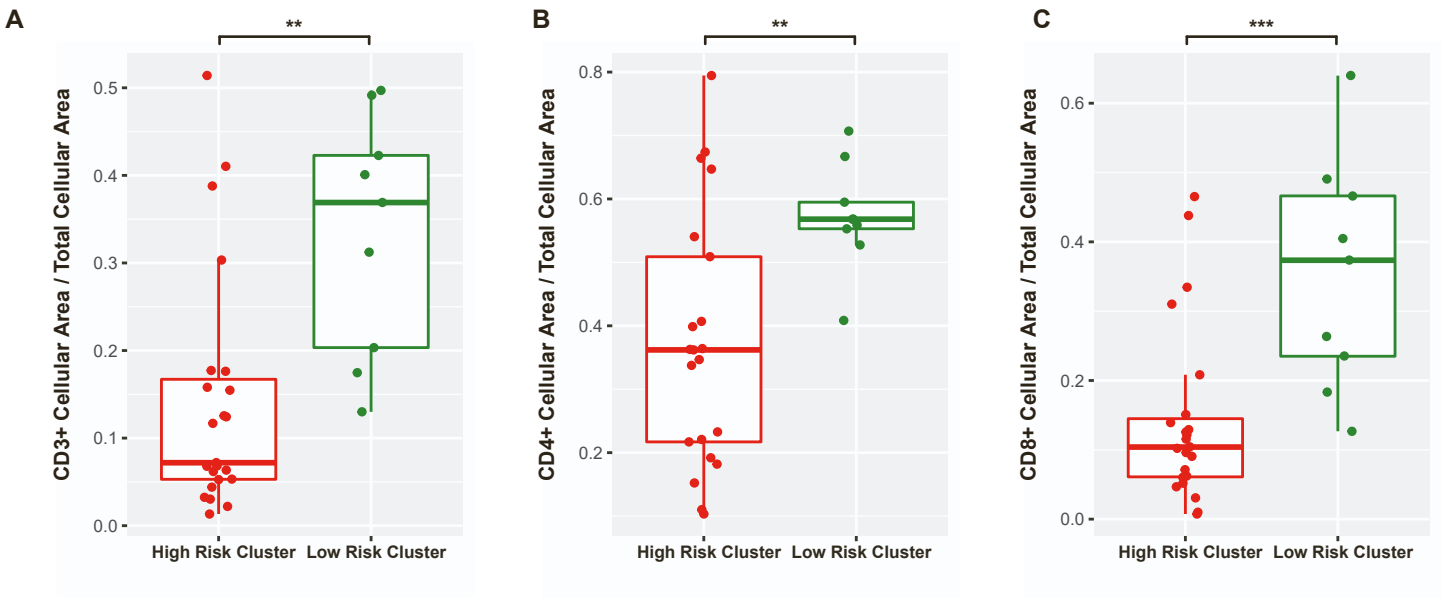
A
**
CD3+ Cellular Area / Total Cellular Area
0.0
0.1
0.2
0.3
0.4
0.5
High Risk Cluster
Low Risk Cluster
B
**
CD4+ Cellular Area / Total Cellular Area
0.2
0.4
0.6
0.8
High Risk Cluster
Low Risk Cluster
C
***
CD8+ Cellular Area / Total Cellular Area
0.0
0.2
0.4
0.6
High Risk Cluster
Low Risk Cluster

Figure S5

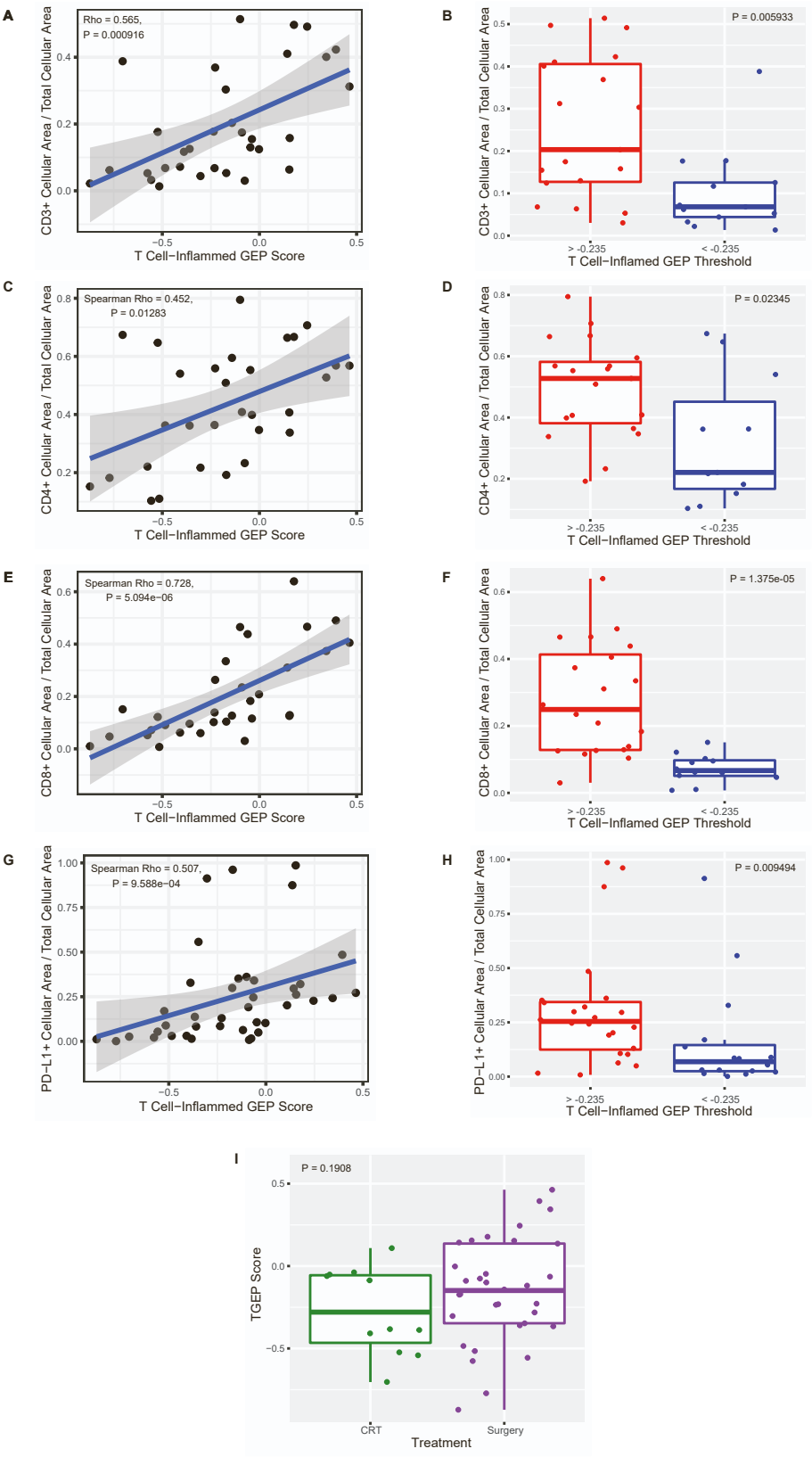
A
Rho = 0.565,
P = 0.000916
CD3+ Cellular Area / Total Cellular Area
T Cell−Inflammed GEP Score
B
P = 0.005933
CD3+ Cellular Area / Total Cellular Area
> -0.235
< -0.235
T Cell−Inflamed GEP Threshold
C
Spearman Rho = 0.452,
P = 0.01283
CD4+ Cellular Area / Total Cellular Area
T Cell−Inflammed GEP Score
D
P = 0.02345
CD4+ Cellular Area / Total Cellular Area
> -0.235
< -0.235
T Cell−Inflamed GEP Threshold
E
Spearman Rho = 0.728,
P = 5.094e−06
CD8+ Cellular Area / Total Cellular Area
T Cell−Inflammed GEP Score
F
P = 1.375e-05
CD8+ Cellular Area / Total Cellular Area
> -0.235
< -0.235
T Cell−Inflamed GEP Threshold
G
Spearman Rho = 0.507,
P = 9.588e−04
PD−L1+ Cellular Area / Total Cellular Area
T Cell−Inflammed GEP Score
H
P = 0.009494
PD−L1+ Cellular Area / Total Cellular Area
> -0.235
< -0.235
T Cell−Inflamed GEP Threshold
I
P = 0.1908
TGEP Score
CRT
Surgery
Treatment

Figure S6

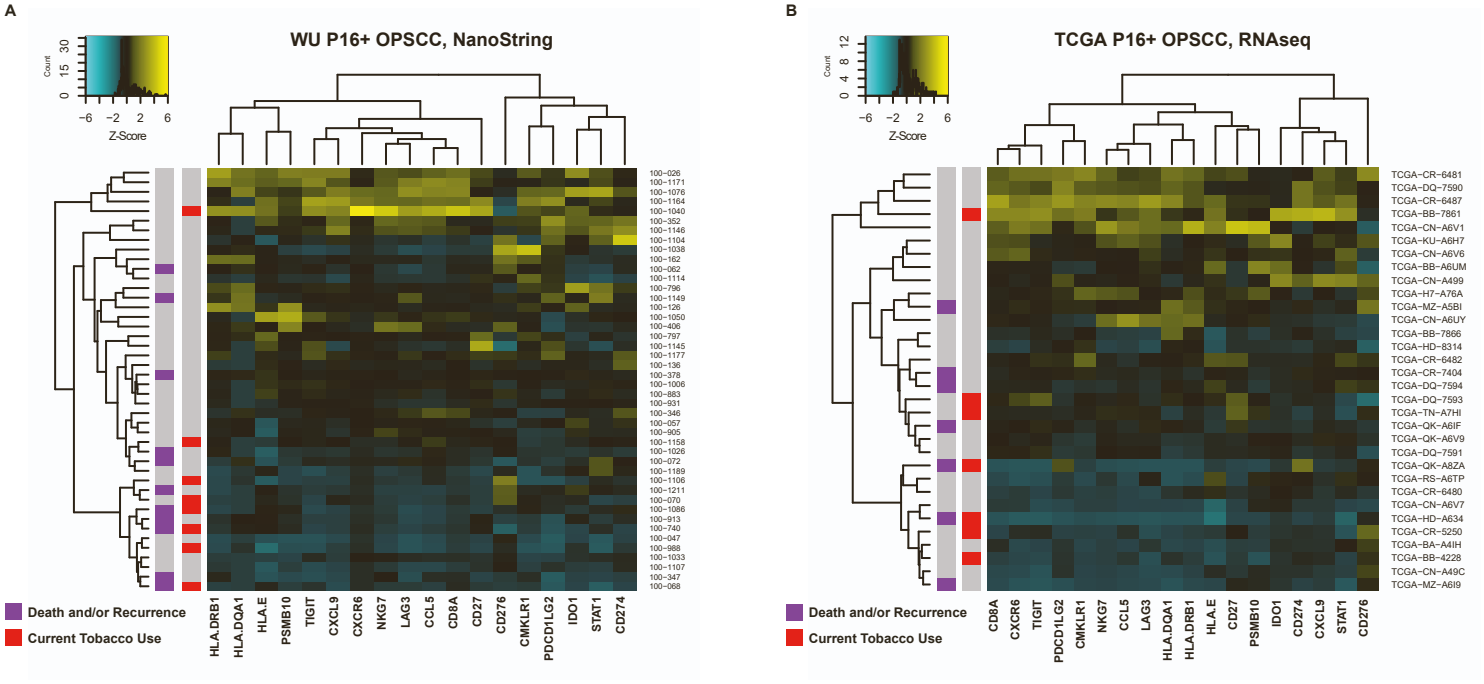
A
WU P16+ OPSCC, NanoString
Count
Z-Score
Death and/or Recurrence
Current Tobacco Use
HLA.DRB1
HLA.DQA1
HLA.E
PSMB10
TIGIT
CXCL9
CXCR6
NKG7
LAG3
CCL5
CD8A
CD27
CD276
CMKLR1
PDCD1LG2
IDO1
STAT1
CD274
B
TCGA P16+ OPSCC, RNAseq
Count
Z-Score
Death and/or Recurrence
Current Tobacco Use
CD8A
CXCR6
TIGIT
PDCD1LG2
CMKLR1
NKG7
CCL5
LAG3
HLA.DQA1
HLA.DRB1
HLA.E
CD27
PSMB10
IDO1
CD274
CXCL9
STAT1
CD276

Figure S7

CD8+ with hematoxylin

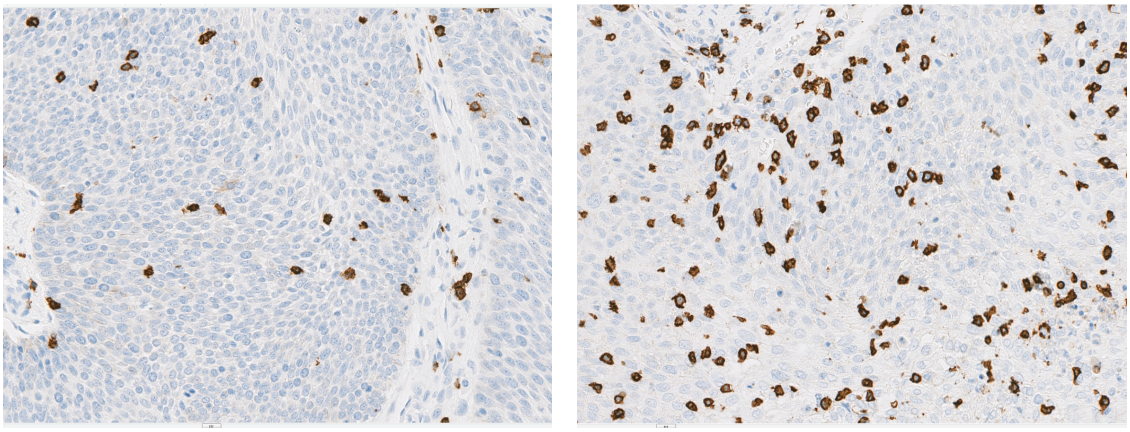

Scored images after RBG filters

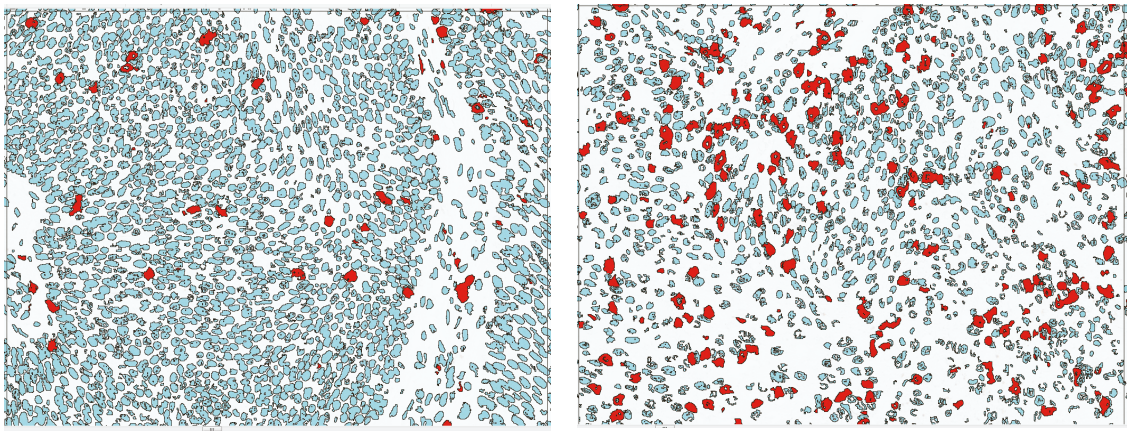

SUPPLEMENTAL FIGURE LEGENDS

Figure S1: Survival analyses for disease stage and tobacco use; related to Table 1. Significant differences in **(A)** OS and **(B)** DFS were present by AJCC 8th Edition Clinical Stage (both Log-rank P < 0.001). No significant differences in **(C)** OS and **(D)** DFS were present by tobacco use history (Log-rank P = 0.220 and 0.650, respectively).

Figure S2: Copy number alterations in HPV(+) OPSCC; related to Figure 1. **(A)** Heatmap displaying copy number alterations for each sample (rows) and chromosome (columns). Clinical annotation is included on the left margin. **(B)** GISTIC plots for focal amplifications and deletions in our cohort.

Figure S3: Tumor mutational burden analysis by clinical features; related to Figure 1. No significant differences in tumor mutational burden were present on the basis of **(A)** tobacco use history or **(B)** disease-free survival at five years (Kruskal-Wallis and Wilcoxon tests, respectively; n.s. = not significant).

Figure S4: IHC confirmation of unsupervised clustering results; related to Figure 4. ORA revealed that gene cluster 4 was significantly enriched for adaptive immune-related pathways. IHC confirmed that the low-risk patient cluster, which had high expression of gene cluster 4, had significantly greater infiltration of **(A)** CD3+, **(B)** CD4+ and **(C)** CD8+ cells. (** Wilcoxon P < 0.01, *** P < 0.001, all FDR < 0.1).

Figure S5: IHC validation of TGEP scores; related to Figure 5. TGEP scores were significantly correlated with IHC staining of **(A)** CD3, **(B)** CD4, and **(C)** PD-L1 (all P < 0.05 and FDR < 0.1). **(D)** No significant differences in TGEP scores were present on the basis of primary treatment modality (primary chemoradiation versus surgery, Welch's T test P = 0.191), suggesting that tissue sourcing (biopsy versus primary surgical specimen) does not represent a source of bias.

Figure S6: Cross-platform comparison of TGEP transcript expression; related to Figure 5. Scaled transcript expression was clustered in **(A)** the study cohort and **(B)** p16(+) OPSCC samples from TCGA, then annotated with current tobacco status and death and/or recurrence.

Figure S7: Representative images of high-resolution digital analysis of IHC staining; related to STAR Methods. Custom red-green-blue (RBG) color filters were programmed which reliably distinguished and quantified areas of 3,3'-diaminobenzidine stained cells (red), hematoxylin stained cells (blue), and acellular background (white) over the entirety of a sample. Example images show original images at 20x magnification (top panels) and the same regions after application of filters (bottom panels).